

Article

# Gate Stability of GaN-Based HEMTs with P-Type Gate

Matteo Meneghini <sup>1,\*</sup>, Isabella Rossetto <sup>1</sup>, Vanessa Rizzato <sup>1</sup>, Steve Stoffels <sup>2</sup>,  
Marleen Van Hove <sup>2</sup>, Niels Posthuma <sup>2</sup>, Tian-Li Wu <sup>2</sup>, Denis Marcon <sup>2</sup>, Stefaan Decoutere <sup>2</sup>,  
Gaudenzio Meneghesso <sup>1</sup> and Enrico Zanoni <sup>1</sup>

<sup>1</sup> Department of Information Engineering, University of Padova, via Gradenigo 6/B, 35131 Padova, Italy; rossett6@dei.unipd.it (I.R.); vanessa.rizzato@dei.unipd.it (V.R.); gauss@dei.unipd.it (G.M.); zanoni@dei.unipd.it (E.Z.)

<sup>2</sup> IMEC, Kapeldreef 75, 3001 Heverlee, Belgium; Steve.Stoffels@imec.be (S.S.); Marleen.VanHove@imec.be (M.V.H.); Niels.Posthuma@imec.be (N.P.); Tian-Li.Wu@imec.be (T.L.W.); Denis.Marcon@imec.be (D.M.); Stefaan.Decoutere@imec.be (S.D.)

\* Correspondence: matteo.meneghini@dei.unipd.it; Tel.: +3904-9827-7664

Academic Editor: Farid Medjdoub

Received: 1 February 2016; Accepted: 15 March 2016; Published: 25 March 2016

**Abstract:** This paper reports on an extensive investigation of the gate stability of GaN-based High Electron Mobility Transistors with p-type gate submitted to forward gate stress. Based on combined electrical and electroluminescence measurements, we demonstrate the following results: (i) the catastrophic breakdown voltage of the gate diode is higher than 11 V at room temperature; (ii) in a step-stress experiment, the devices show a stable behavior up to  $V_{GS} = 10$  V, and a catastrophic failure happened for higher voltages; (iii) failure consists in the creation of shunt paths under the gate, of which the position can be identified by electroluminescence (EL) measurements; (iv) the EL spectra emitted by the devices consists of a broad emission band, centered around 500–550 nm, related to the yellow-luminescence of GaN; and (v) when submitted to a constant voltage stress tests, the p-GaN gate can show a time-dependent failure, and the time to failure follows a Weibull distribution.

**Keywords:** gallium nitride; high electron mobility transistor; degradation; step stress

## 1. Introduction

Gallium nitride transistors have recently been demonstrated to be excellent devices for application in the power electronics field. Thanks to the high breakdown voltage of GaN (3.3 MV/cm), high electron mobility transistors (HEMTs) can reach breakdown voltages in excess of 1 kV; in addition, the high mobility of the electrons in the channel results in a low on-resistance. With regard to this last aspect, recent on-resistance values reported in the literature are 100 m $\Omega$  for a 20 A/650 V transistors [1], 70 m $\Omega$  for 600 V AlGaIn/GaN devices with a 214  $\mu$ m gate width [2], and a specific on-resistance of 2.3 m $\Omega$  cm<sup>2</sup> for normally-off devices with a gate-drain distance of 12  $\mu$ m [3]. Finally, the wide bandgap of the semiconductor (3.4 eV) allows for high temperature operation.

The high electron density in the two-dimensional electron gas (2DEG) is obtained thanks to the spontaneous and piezoelectric polarization of GaN, without the need for any doping; typically, GaN-based transistors are normally-on devices, with a negative threshold voltage. Several methods have been recently proposed for the fabrication of normally-off GaN-based transistors: the use of a deep gate recess, in combination with a metal-insulator-semiconductor (MIS) stack [4]; the implantation of fluorine ions under the gate [5], that results in a significant depletion of the channel; the use of a p-type gate material, such as p-AlGaIn [6] or p-GaN [7], which shifts the conduction band upwards, thus resulting in the depletion of the channel for negative gate voltages. As an alternative to these strategies,

it has been also proposed to develop special E-mode devices, integrating a normally-on GaN HEMT connected in cascode configuration to a normally-off silicon MOSFET (Metal Oxide Semiconductor Field Effect Transistor) in the same package [8]. In this last approach, the on/off state of the low-voltage silicon MOSFET controls the on/off state of the GaN-based high voltage HEMT; the cascoded device behaves then as an enhancement device, which is compatible with commercial drivers. All of these approaches have advantages and drawbacks: the use of a gate recess with gate insulator leads to a very low gate leakage current, but can favor trapping at the interfaces and/or in the insulator, as well as time-dependent dielectric breakdown; fluorine implantation allows to obtain high (positive) threshold voltages ( $>2$  V, [9]), but the fluorine ions (and the threshold voltage) can be unstable if the devices are submitted to long-term stress [10]); the use of a p-type gate requires the optimization and activation of the p-type dopant (magnesium), *i.e.*, an additional growth step; finally, cascoded HEMTs are rather complex structures, having two devices mounted on the same package. This can generate reliability problems, due to the use of extra bonding wires, and to the fact that a silicon-based transistor is used in proximity of a GaN HEMT that—in principle—can operate at high temperatures.

Several reports on the reliability of MIS-based devices and normally-on HEMTs have already been published in the literature (see, for instance, [11,12] and references therein). On the other hand, only little information on the stability of HEMTs with a p-gate is currently available [13,14].

The aim of this paper is to contribute to the understanding of the physical mechanisms responsible for the failure of GaN-based HEMTs with p-GaN gate submitted to positive bias stress. We present our recent results on the degradation of transistors with a p-GaN gate submitted to stress with positive gate voltage. The results of our investigation indicate that the analyzed devices have a (positive) breakdown voltage higher than 11 V at room temperature, and can show a catastrophic failure when they are submitted to a step-stress experiment. Information on the nature of the failure mechanism is provided based on spatially- and spectrally-resolved electroluminescence (EL) measurements and on optical characterization. Finally, we demonstrate the existence of a time-dependent breakdown process in positively-biased devices with p-GaN gate.

## 2. Materials and Methods

The analysis was carried out on HEMTs with p-GaN gate, whose structure is schematically represented in Figure 1. The devices were grown by metal-organic chemical vapour deposition on a 200 mm silicon substrate; the epitaxial structure consists of a 200 nm AlN nucleation layer, a 1  $\mu\text{m}$  AlGaN backbarrier, a 2  $\mu\text{m}$  AlGaN buffer layer, a 300 nm GaN channel layer, a 15 nm  $\text{Al}_{0.25}\text{Ga}_{0.75}\text{N}$  barrier, and a 70 nm p-GaN layer. This study is aimed at investigating the stability and degradation of the p-GaN gate under positive bias conditions. All the measurements were carried out on symmetric test structures without field plate, that allow to observe the gate from the top during the execution of the electroluminescence measurements. The gate width is  $W_G = 100 \mu\text{m}$ , and the gate length is  $L_G = 0.8 \mu\text{m}$ . The electrical measurements were carried out in a probe station equipped with a semiconductor parameter analyzer (Keysight B1505). The electroluminescence characterization was carried out by means of a high-sensitivity Si-based camera (Luca Andor, UK), mounted on an optical microscope with visible-ultraviolet lenses (Mitutoyo, Japan); the synchronization between the electrical stimulus and the camera was obtained through a customized LabView<sup>®</sup> software (LabView 2009, National Instruments, USA).

The electrical characteristics measured on a representative device are plotted in Figure 2; the threshold voltage is  $V_{\text{TH}} = 1.7$  V (at 100  $\mu\text{A}/\text{mm}$ ,  $V_{\text{DS}} = 1$  V), and at higher drain voltages remains well above 1 V ( $V_{\text{TH}} = 1.32$  V at 100  $\mu\text{A}/\text{mm}$ ,  $V_{\text{DS}} = 10$  V).

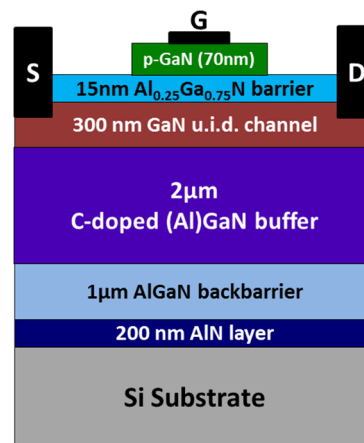


Figure 1. Schematic structure of the samples analyzed within this paper.

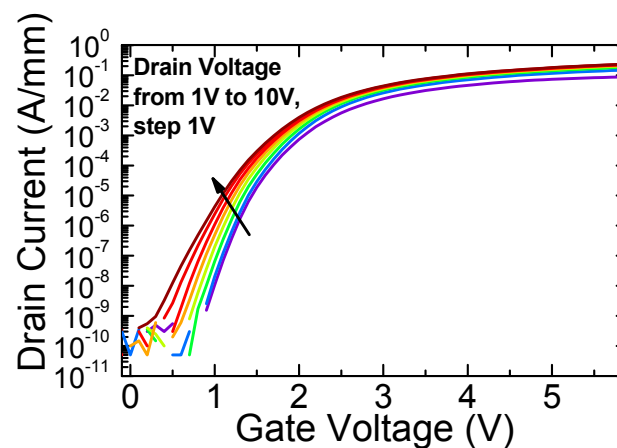
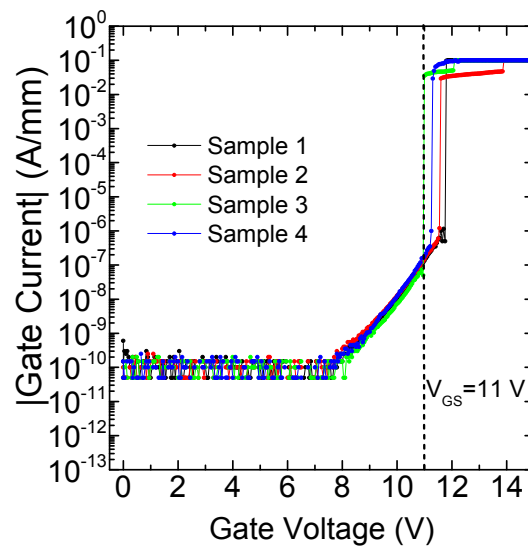


Figure 2. Drain current vs gate voltage curves measured on one of the analyzed devices for different drain voltages.

### 3. Results

Before starting with the stress experiments, the devices were preliminary submitted to a breakdown stress. The gate voltage was rapidly swept from 0 V to 15 V, and the corresponding gate current was monitored. During the measurement, the drain, source and chuck were grounded. Representative results obtained on four identical samples are reported in Figure 3. As can be noticed, the gate current is negligible and below instrument sensitivity (around 100 pA/mm) up to a gate voltage of 8 V (the gate voltage swing of these devices is 6 V). For gate voltages between 8 V and 11 V, gate current shows an exponential increase, reaching values in the order of 100 nA/mm. For higher voltages, the devices reach the forward gate breakdown, that corresponds to a rapid increase in gate leakage. This degradation is permanent (*i.e.*, not recoverable), and—once the devices have reached the breakdown—the gate current is around 10–100 mA/mm for voltages higher than 12 V.

In a dc breakdown test, the device fails rapidly, so it is impossible to investigate the physical origin of the degradation. To obtain a better description of the degradation process, we carried out a series of step-stress experiments: the stress voltage applied to the gate was increased by 0.5 V every 120 s, with source, drain and chuck grounded. The gate current was constantly monitored during stress, together with the electroluminescence signal emitted by the devices.



**Figure 3.** Forward-voltage breakdown curves measured on 4 representative devices.

The results obtained on one of the analyzed samples are reported in Figure 4. Gate current remains below the instrumentation limit up to a stress voltage of  $V_{GS} = 7.0$  V. During the subsequent steps (for  $7.5 \text{ V} < V_{GS} < 9.5 \text{ V}$ ), the gate current slightly increases during each stage of the step-stress experiment. The failure is reached during the step at  $V_{GS} = 10$  V; after an initial phase in which current increases slowly with time, gate leakage shows a rapid increase and reaches the compliance limit.

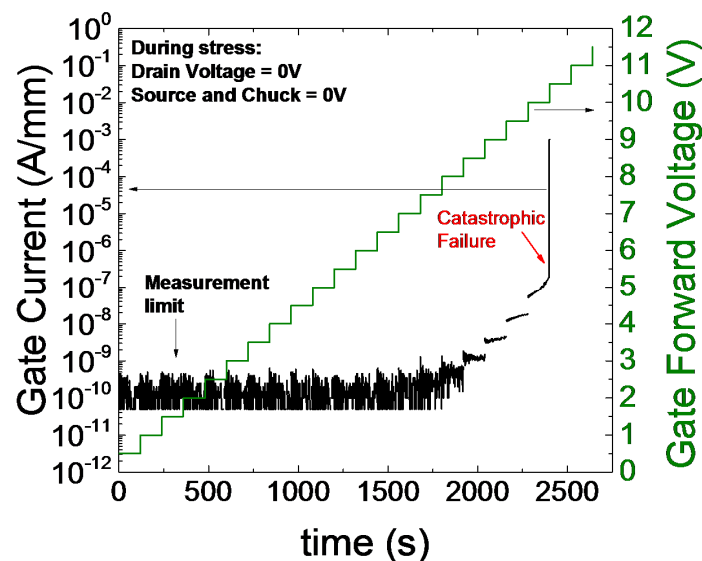


**Figure 4.** Results of a step-stress experiment carried out on one of the analyzed devices. With drain and source grounded, the gate voltage is increased by 0.5 V every 120 s. The corresponding gate current is sampled every second.

The spatially-resolved electroluminescence measurements carried out before and during the step-stress experiment showed negligible light emission up to  $V_{GS} = 9$  V (Figure 5a); this result is consistent with the very low gate leakage detected in this voltage range. Remarkably, during the step at  $V_{GS} = 10$  V a weak luminescence signal was detected (Figure 5b). Under these conditions light emission is focused in proximity of three localized regions, and stronger in the area indicated by the white arrow in Figure 5b. After failure (and after the corresponding increase in gate leakage), forward

current flows mostly in a localized area located in proximity of the dominant emission spot identified before failure (compare Figure 5b,c).

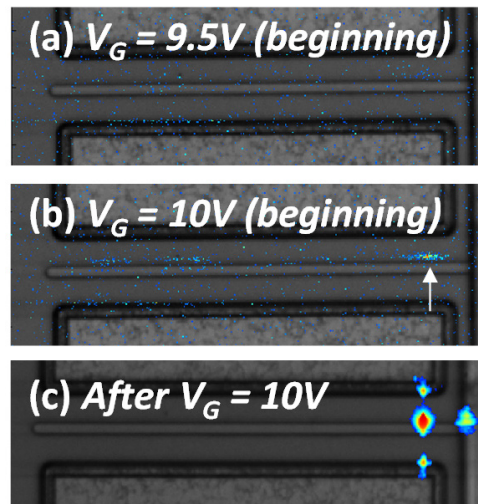


**Figure 5.** Spatially-resolved electroluminescence measurements carried out along the gate of the analyzed devices (a) at the beginning of the stress at  $V_{GS} = 9.5$  V, (b) at the beginning of the stress at  $V_{GS} = 10$  V and (c) after the catastrophic failure.

More detailed data on the origin of the luminescence signal were collected by means of spectrally-resolved electroluminescence measurements. The EL spectra were measured on the same sample of Figure 5 (after stress) by applying a constant gate current of 1 mA to the gate of the devices. The measurements were carried out by means of a high sensitivity cooled CCD (charge-coupled device) camera equipped with a monochromator. Figure 6 reports the EL spectra emitted by the same sample as in Figure 5. The device emits a broad luminescence peak centered around 500–550 nm. The origin of luminescence can be explained by considering that—under high forward bias—a high current of energetic electrons flows through the p-GaN/i-AlGaN junction. The flow of highly energetic electrons can induce the ionization of the deep levels responsible for the yellow luminescence of GaN (consistently with [13,15,16]). It is worth noticing that the gate voltage of the devices remains stable during the whole duration of the EL spectral measurements (see Figure 6), demonstrating that the spectral measurement does not induce any further degradation.

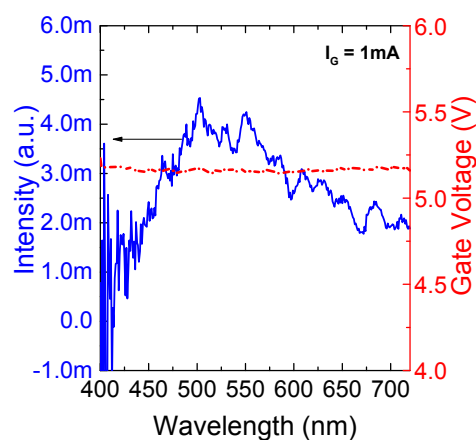


**Figure 6.** EL (electroluminescence) spectra evaluated from  $\lambda = 400$  nm to  $\lambda = 720$  nm on the same device as Figure 5 after the stepstress. The gate voltage measured during the acquisition of each wavelength is also reported.

The results collected during the last stage of the stress step experiment in Figure 4 indicate that the catastrophic degradation does not occur immediately after the stress is applied, but after several seconds of operation at  $V_{GS} = 10$  V. This result suggests that the devices show a time-dependent failure. To better investigate this aspect, we carried out a set of constant voltage stress tests at voltages close to (but smaller than) the dc breakdown voltage. Figure 7 reports the results obtained by stressing identical samples with a gate voltage of 9.75 V, and source, drain, and chuck grounded. As can be noticed, in the initial phase of the stress experiment the gate current is very low and stable; this phase is followed by a gradual increase in gate leakage, that—for most of the samples—changes of 2–3 orders of magnitude. Failure occurs as a sudden increase in gate leakage (reaching the compliance value of 10 mA/mm).

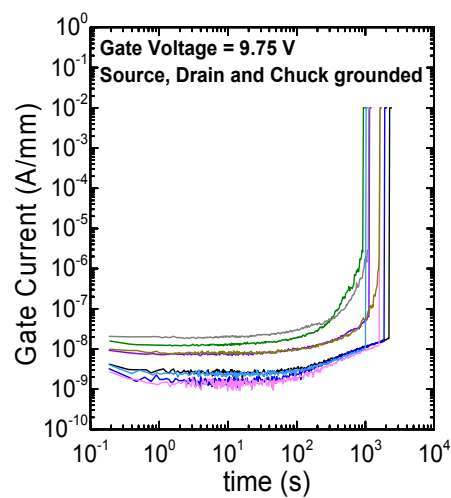


**Figure 7.** Results of constant voltage stress tests carried out on eight identical devices with a gate bias of 9.75 V, source, drain and substrate connected to ground.

The time-to-failure was found to follow a Weibull distribution (Figure 8), with a shape factor  $\beta$  of 2.25 (indicating that the failure rate increases with time) and a scale parameter (time at which 63.2% of samples failed)  $\eta$  of 1454 s. The time to failure is supposed to become shorter with increasing stress voltages. By analyzing the mean time to failure during stress at different voltage levels, we estimated that the devices have a twenty-years lifetime for a gate voltage of 7.2 V; this value is significantly higher than the typical gate operating voltage (5 V).

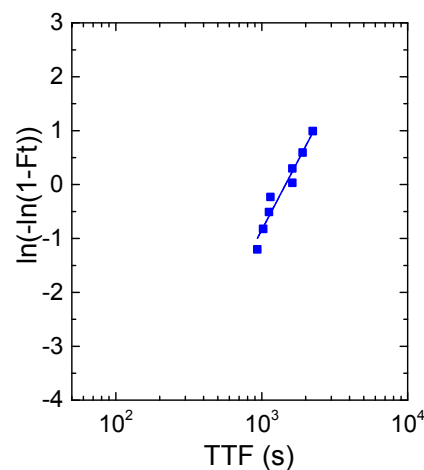


**Figure 8.** Weibull distribution of time-to-failure for the analyzed devices.  $\beta = 2.25$ ,  $\eta = 1454$  s.



The time-dependent failure process described above can be interpreted based on the following considerations. In reverse-biased Schottky junctions, the time-dependent failure has been ascribed to the degradation of the AlGa<sub>N</sub> layer, that is subject to a high electric field [15,17]. However, the devices analyzed within this paper are submitted to a positive gate bias, and 2D simulations [13] demonstrate that the absolute value of the electric field in the AlGa<sub>N</sub> decreases significantly during stress, with respect to rest conditions. The observed failure can therefore not be ascribed to the degradation of the AlGa<sub>N</sub> barrier.

Two other mechanisms can therefore be considered:

- (i) at high (positive) gate bias, the electric field in the p-GaN can significantly increase (see the simulations in [13]), since the Schottky metal/p-GaN diode is reversely biased and the p-GaN is partly depleted. The high electric field can favor the generation of defects in the p-GaN, similarly to what observed in the AlGa<sub>N</sub> barrier under negative bias [15,18,19]. This may lead the generation of leakage paths and to the consequent failure of the gate junction. Avalanche effects (proposed in [13]) can further accelerate the defect generation process.
- (ii) during positive voltage stress the Si<sub>3</sub>N<sub>4</sub> passivation may be exposed to a high electric field, especially in proximity of the gate edge. This may lead to a time-dependent (and geometry-dependent) dielectric failure of Si<sub>3</sub>N<sub>4</sub>, with consequent increase in gate leakage.

#### 4. Conclusions

In summary, in this paper we have described an analysis of the degradation mechanisms of GaN-HEMTs with p-type gate submitted to positive bias stress. The results demonstrate that in the operating voltage range (up to 7 V) the devices have an high robustness towards stress. In addition, based on the results of dc breakdown measurements, step-stress experiment and constant voltage tests, we demonstrated that the transistors can show a time-dependent failure when submitted to forward gate stress at higher voltages ( $V_{GS} > 9$  V). The failure corresponds to an increase in gate leakage, that is well correlated to the generation of hot-spots, identified by means of EL measurements. Possible mechanisms responsible for this failure have been discussed based on the experimental evidence collected within this paper.

**Acknowledgments:** This project has received funding from the Electronic Component Systems for European Leadership Joint Undertaking under grant agreement No 662133. This Joint Undertaking receives support from the European Union's Horizon 2020 research and innovation programme and Austria, Belgium, Germany, Italy, Netherlands, Norway, Slovakia, Spain, United Kingdom. This article reflects only the authors' view and the JU is not responsible for any use that may be made of the information it contains.



**Conflicts of Interest:** The authors declare no conflict of interest.

#### References

1. Moens, P.; Banerjee, A.; Uren, M.J.; Meneghini, M.; Karboyan, S.; Chatterjee, I.; Vanmeerbeek, P.; Căsar, M.; Liu, C.; Salih, A.; *et al.* Impact of buffer leakage on intrinsic reliability of 650 V AlGa<sub>N</sub>/Ga<sub>N</sub> HEMTs. In Proceedings of the 2015 IEEE International Electron Devices Meeting, Washington, DC, USA, 7–9 December 2015; pp. 903–906.
2. Hilt, O.; Zhytnytska, R.; Böcker, J.; Bahat-treidel, E.; Brunner, F.; Knauer, A. 70 mΩ/600 V normally-off Ga<sub>N</sub> transistors on SiC and Si substrates. In Proceedings of the 2015 IEEE 27th International Symposium on Power Semiconductor Devices & IC's, Hong Kong, China, 10–14 May 2015; pp. 237–240.
3. Ishida, M.; Ueda, T.; Tanaka, T.; Ueda, D. Ga<sub>N</sub> on Si technologies for power switching devices. *IEEE Trans. Electron. Devices* **2013**, *60*, 3053–3059. [[CrossRef](#)]

4. Wu, T.; Marcon, D.; de Jaeger, B.; van Hove, M.; Bakeroot, B.; Lin, D.; Kang, X.; Roelofs, R.; Groeseneken, G.; Decoutere, S. The impact of the gate dielectric quality in developing Au-free D-mode and E-mode recessed gate AlGaIn/GaN transistors on a 200mm Si substrate. In Proceedings of the 2015 IEEE 27th International Symposium on Power Semiconductor Devices & IC's, Hong Kong, China, 10–14 May 2015; pp. 225–228.
5. Chen, K.J.; Yuan, L.; Wang, M.J.; Chen, H.; Huang, S.; Zhou, Q.; Zhou, C.; Li, B.K.; Wang, J.N. Physics of fluorine plasma ion implantation for GaN normally-off HEMT technology. In Proceedings of the IEEE International Electron Devices Meeting, Washington, DC, USA, 5–7 December 2011; pp. 465–468.
6. Uemoto, Y.; Hikita, M.; Ueno, H.; Matsuo, H.; Ishida, H.; Yanagihara, M.; Ueda, T.; Tanaka, T.; Ueda, D. Gate injection transistor (GIT)—A normally-off AlGaIn/GaN power transistor using conductivity modulation. *IEEE Trans. Electron. Devices* **2007**, *54*, 3393–3399. [[CrossRef](#)]
7. Zanandrea, A.; Bahat-Treidel, E.; Rampazzo, F.; Stocco, A.; Meneghini, M.; Zanoni, E.; Hilt, O.; Ivo, P.; Wuerfl, J.; Meneghesso, G. Single- and double-heterostructure GaN-HEMTs devices for power switching applications. *Microelectron. Reliab.* **2012**, *52*, 2426–2430. [[CrossRef](#)]
8. Huang, X.; Liu, Z.; Li, Q.; Lee, F.C. Evaluation and application of 600 v GaN HEMT in cascode structure. *IEEE Trans. Power Electron.* **2014**, *29*, 2453–2461. [[CrossRef](#)]
9. Liu, C.; Wang, H.; Yang, S.; Lu, Y.; Liu, S.; Tang, Z.; Jiang, Q.; Huang, S.; Chen, K.J. Normally-off GaN MIS-HEMT with improved thermal stability in DC and dynamic performance. In Proceedings of the 2015 IEEE 27th International Symposium on Power Semiconductor Devices & IC's, Hong Kong, China, 10–14 May 2015; pp. 213–216.
10. Bisi, D.; Meneghini, M.; Stocco, A.; Cibin, G.; Pantellini, A.; Nanni, A.; Lanzieri, C.; Zanoni, E.; Meneghesso, G. Influence of fluorine-based dry etching on electrical parameters of AlGaIn/GaN-on-Si high electron mobility transistors. In Proceedings of the European Solid-State Device Research Conference, Bucharest, Romania, 16–20 September 2013; pp. 61–64.
11. Meneghini, M.; Member, S.; Rossetto, I.; Hurkx, F.; Šonský, J.; Croon, J.A.; Meneghesso, G.; Zanoni, E. Extensive Investigation of time-dependent breakdown of GaN-HEMTs submitted to OFF-state stress. *IEEE Trans. Electron. Devices* **2015**, *62*, 2549–2554. [[CrossRef](#)]
12. Wu, T.; Marcon, D.; de Jaeger, B.; van Hove, M.; Bakeroot, B.; Stoffels, S.; Groeseneken, G.; Decoutere, S.; Roelofs, R. Time dependent dielectric breakdown (TDDB) evaluation of PE-ALD SiN gate dielectrics on AlGaIn/GaN recessed gate D-mode MIS-HEMTs and E-mode MIS-FETs. In Proceedings of the IEEE International Reliability Physics Symposium, Monterey, CA, USA, 19–23 April 2015; pp. 4–9.
13. Wu, T.; Member, S.; Marcon, D.; You, S.; Posthuma, N.; Bakeroot, B.; Stoffels, S.; van Hove, M.; Groeseneken, G.; Decoutere, S. Forward bias gate breakdown mechanism in enhancement-mode p-GaN gate AlGaIn/GaN high-electron mobility transistors. *IEEE Electron. Device Lett.* **2015**, *36*, 1001–1003. [[CrossRef](#)]
14. Ľapajna, M.; Hilt, O.; Würfl, J.; Kuzmík, J. Investigation of gate-diode degradation in normally-off p-GaN/AlGaIn/GaN high-electron-mobility transistors. *Appl. Phys. Lett.* **2015**, *107*. [[CrossRef](#)]
15. Meneghini, M.; Stocco, A.; Bertin, M.; Marcon, D.; Chini, A.; Meneghini, M.; Stocco, A.; Bertin, M.; Marcon, D.; Chini, A.; *et al.* Time-dependent degradation of AlGaIn/GaN high electron mobility transistors under reverse bias. *Appl. Phys. Lett.* **2012**, *100*. [[CrossRef](#)]
16. Meneghesso, G.; Rossi, F.; Salviati, G.; Uren, M.J.; Muoz, E.; Zanoni, E. Correlation between kink and cathodoluminescence spectra in AlGaIn/GaN high electron mobility transistors. *Appl. Phys. Lett.* **2010**, *96*, 10–13. [[CrossRef](#)]
17. Joh, J.; Gao, F.; Palacios, T.; del Alamo, J.A. A model for the critical voltage for electrical degradation of GaN high electron mobility transistors. *Microelectron. Reliab.* **2010**, *50*, 767–773. [[CrossRef](#)]
18. Marcon, D.; Viaene, J.; Favia, P.; Bender, H.; Kang, X.; Lenci, S.; Stoffels, S.; Decoutere, S. Reliability of AlGaIn/GaN HEMTs: Permanent leakage current increase and output current drop. In Proceedings of the International Symposium on the Physical and Failure Analysis of Integrated Circuits (IPFA), Suzhou, China, 15–19 July 2013; pp. 249–254.
19. Marcon, S.D.D.; Meneghesso, G.; Wu, T.L.; Stoffels, S.; Meneghini, M. Reliability analysis of permanent degradations on AlGaIn/GaN HEMTs. *IEEE Trans. Electron. Devices* **2013**, *60*, 3132–3141. [[CrossRef](#)]

